energies

MDPI

Article

Effect of Iron Oxide Nanoparticles on the Properties of Water-Based Drilling Fluids

Muhammad Awais Ashfaq Alvi [1,*], Mesfin Belayneh [1], Sulalit Bandyopadhyay [2] and Mona Wetrhus Minde [3]

[1] Department of Energy and Petroleum Engineering, University of Stavanger, N-4036 Stavanger, Norway; mesfin.a.belayneh@uis.no
[2] Department of Chemical Engineering, Norwegian University of Science and Technology (NTNU), N-7491 Trondheim, Norway; sulalit.bandyopadhyay@ntnu.no
[3] Department of Mechanical, Structural Engineering and Materials Science, University of Stavanger, N-4036 Stavanger, Norway; mona.w.minde@uis.no
* Correspondence: muhammad.a.alvi@uis.no or aawaisalvi@gmail.com

Received: 24 November 2020; Accepted: 16 December 2020; Published: 19 December 2020

Abstract: In recent years, several studies have indicated the impact of nanoparticles (NPs) on various properties (such as viscosity and fluid loss) of conventional drilling fluids. Our previous study with commercial iron oxide NPs indicated the potential of using NPs to improve the properties of a laboratory bentonite-based drilling fluid without barite. In the present work, iron oxide NPs have been synthesized using the co-precipitation method. The effect of these hydrophilic NPs has been evaluated in bentonite and KCl-based drilling fluids. Rheological properties at different temperatures, viscoelastic properties, lubricity, and filtrate loss were measured to study the effect of NPs on the base fluid. Also, elemental analysis of the filtrate and microscale analysis of the filter cake was performed. Results for bentonite-based fluid showed that 0.019 wt% (0.1 g) of NPs reduced the coefficient of friction by 47%, and 0.0095 wt% (0.05 g) of NPs reduced the fluid loss by 20%. Moreover, for KCl-based fluids, 0.019 wt% (0.1 g) of additive reduced the coefficient of friction by 45%, while higher concentration of 0.038 wt% (0.2 g) of NPs shows 14% reduction in the filtrate loss. Microscale analysis shows that presence of NPs in the cake structure produces a more compact and less porous structure. This study indicates that very small concentration of NPs can provide better performance for the drilling fluids. Additionally, results from this work indicate the ability of NPs to fine-tune the properties of drilling fluids.

Keywords: drilling fluids; nanoparticles; iron oxide; KCl; bentonite drilling fluids

1. Introduction

Drilling is the process of connecting the surface to the reservoir. In a rotary drilling operation, drilling fluids play an important role in maintaining well pressure, bringing cuttings to surface, and lubricating and cooling drill bits as well as the wellbore [1,2]. Proper selection of the drilling fluid is one of the key elements for the success of drilling operation. The selection of drilling fluid is usually based on its performance, cost and environmental impact [2].

Due to the interactions between the drilling fluid and the rock, a poorly designed drilling fluid may cause formation damage. The consequences are a negative impact on the log reading and damage to the pore space of the reservoir rock, that reduces its productivity. Increase in fluid loss into the formation will increase the near bore pressure, which as a result will weaken the strength of the wellbore. Moreover, drilling with non-inhibitive water-based drilling fluids will result in shale swelling. If the drilling fluid is poor at holding particles in suspension, cuttings will be accumulated in the

wellbore and result in solid-induced drill string stuck. Also, the thick mud cake may cause differential sticking problems [3,4].

Therefore, in general, drilling fluid design is one of the most important aspects to consider during the well construction and completion phases. The drilling fluid parameters under consideration, among others, are the rheological properties to control the hydraulics (well pressure and hole cleaning), lubricity to control the high torque and drag issues, mud cake properties to control fluid loss and to increase well strength [5,6]. The properties of drilling fluids are determined by the types and the concentration of the chemical additives used in their formulations. The right parameters must be characterized experimentally, and several formulation iterations may be required until the desired properties are achieved.

Typically, water- and oil-based drilling fluids, also known as water-based mud (WBM) and oil-based mud (OBM), are used in oil and gas wells [7]. In terms of lubricity and formation damage control, OBM is better than WBM [8]. The application of OBM is limited in environmentally sensitive areas, and hence, only drilling with water-based fluids is allowed. Moreover, WBM is used to drill the top-hole section where there is no blowout preventer (BOP) in place and drilling fluids can be discharged to the seabed. However, WBM still requires further improvement to provide better lubricity, shale inhibition, and formation damage control.

In recent years, several researchers have reported the impact of nanoparticles (NPs) on the properties of water-based drilling fluids. Studies indicate that the addition of NPs can alter the rheological parameters of drilling fluids under low pressure/low temperature (LPLT) and high pressure/high temperature (HPHT) conditions [9–15], reduce filtrate loss and filter cake thickness [9,16–20], reduce friction [13,15,16,21,22], improve thermal conductivity and heat transfer properties [17,20,23,24] and shale inhibition and wellbore strengthening [25–28]. Iron-based NPs have been added to water-based drilling fluids in several studies. For instance, Jung et al. [29] showed that the addition of iron oxide NPs to a bentonite-based fluid increases the viscosity of the fluid. This study indicated that the NPs interacted with the bentonite and promoted the gelation of the clay particles. In addition, a low concentration of NPs reduces the LPLT fluid loss values of the fluid, however increasing the concentration of NPs results in lesser reduction in fluid loss. Barry et al. [30] also investigated the effect of iron oxide on bentonite drilling fluids and observed higher values of shear stress with the addition of NPs compared to the base fluid. Addition of iron oxide particles at a concentration of 0.5 wt% and with sizes of 3 nm and 30 nm to the bentonite suspension reduced the fluid loss by 27% and 23.4%, respectively. Drilling fluids containing commercial iron oxide were also investigated by Mahmoud et al. [31]. Different concentrations of NPs were tested in this study with, a suspension of Ca-bentonite having 7 wt% concentration as a base fluid. The findings from this work illustrated that yield point and plastic viscosity were changed by the addition of iron oxide NPs to the drilling fluid. In order to enhance the filtration and rheological properties of Na-bentonite-based drilling fluids, Vryzas et al. [32,33] explored some novel iron oxide NPs. These studies illustrated that the apparent viscosity and yield stress become progressively susceptible to the temperature. An increase in apparent viscosity and yield stress was observed at a higher temperature. Moreover, 0.5 wt% of iron oxide NPs reduced the filtrate loss by 40% compared to the base fluid at high pressure and temperature. Recently, Mahmoud et al. [34,35] added iron oxide to a calcium bentonite-based drilling fluid. Addition of 0.5 wt% NPs to the base fluid decreased the fluid loss and produced a filter cake with better packing characteristics under static and dynamic conditions. In addition, the NPs increased the yield strength and gel-forming ability of the drilling fluid.

Our previous study showed the effect of commercial iron oxide NPs on a bentonite/polymer system in the presence of KCl salt [36]. Results from this study showed that NPs can reduce the friction of the drilling fluid. However, barite was not present in the fluid system. Therefore, in this study, the effects of NPs have been studied on a drilling fluid with barite. Further, most of the studies mentioned above focused on bentonite-based fluids, and not many studies available that studied the effect of NPs on KCl-based drilling fluids. Thus, KCl-based fluids without any bentonite were also

prepared as they are effective for shale-based formations. The potassium in KCl inhibits shale swelling by cation exchange with the calcium present in the shale and by reducing the hydration tendency of the shale [37]. Hence, this study focused on both KCl- and bentonite-based drilling fluid with barite.

2. Materials and Methods

Iron (II) chloride tetrahydrate ($FeCl_2{\cdot}4H_2O$) (Arcos Organics, Thermofisher Scientific, (Oslo, Norway), Iron (III) chloride hexahydrate ($FeCl_3{\cdot}6H_2O$) and ammonia solution (NH_4OH, 25%) were purchased from Sigma Aldrich (Oslo, Norway) and KCl salt was purchased from VWR Chemicals (Oslo, Norway). Bentonite, barite, xanthan gum and soda ash were provided by a drilling fluid service company. De-ionized water was used for al sample preparations.

2.1. Synthesis of Iron Oxide NPs

NPs were synthesized by conventional co-precipitation of Fe ions in an alkaline environment [38]. First, 84.6 mL of de-ionized water was weighed in a beaker, and to this de-ionized water, 15.4 mL of 25% ammonia solution was added to make 100 mL of 1 M NH_4OH solution. Separately, 2.0 g of $FeCl_2{\cdot}4H_2O$ and 5.4 g of $FeCl_3{\cdot}6H_2O$ was dissolved in 25 mL distilled water in a volumetric flask. Afterward, 10 mL of this rusty coloured solution was transferred to a burette. The solution was then added dropwise into 100 mL of 1 M NH_4OH solution under vigorous stirring. A magnetic stirrer was used. The addition of the iron solution to the ammonia solution resulted in a black coloured solution. After the reaction was completed, the black coloured solution was transferred to centrifuge tubes. A strong magnet was placed under the centrifuge tubes to separate the particles magnetically, and the particles were washed several times with water. The process was repeated to harvest all the particles. Some NPs might stick to the magnetic stirrer. Therefore, it is essential to wash it several times to recover as many particles as possible. Almost clear fluid was obtained as NPs were drawn to a strong magnet after the first cleaning steps of particles with water. However, after several washes with de-ionized water, the particle's separation becomes difficult as less transparent fluid was obtained when a magnet was placed under the solution. It is crucial to stop washing after it gets difficult to avoid the loss of particles.

2.2. Coating of Xanthan Gum on Iron Oxide NPs (Fe-XG)

To coat xanthan gum polymer on iron oxide NPs, a 0.1 g of xanthan gum was added into 50 mL water to make a polymer solution. Afterward, 0.2 g of iron oxide NPs were added to this polymer solution, and the resulting mixture was left for shaking for 24 h. After 24 h, the resulting solution was used to formulate drilling fluid. The term Fe-XG is used for iron oxide NPs coated with xanthan gum throughout the text.

2.3. Formulation of Drilling Fluid

Two types of water-based fluids were formulated, a bentonite-based fluid and a KCl-based fluid. The fluid compositions were selected to produce fluids having comparable viscosity and density [39]. Tables 1 and 2 show the recipes used for both fluids. First base fluids were formulated, and to these fluids, different concentrations of NPs were added to see the effect of NPs on base fluids. In order to prepare bentonite fluid, all chemicals, excluding barite, were mixed with a Hamilton Beach mixer for 5 min followed by additional 5 min mixing to dislodge any material attached to the mixing container's side. Afterward, barite was added and mixed for 5 min and additional 5 min to dislodge adhering materials to attain the uniform mixing of components. To the base fluid, different concentrations of NPs (0.05–0.2 g) were added and again mixed for 5 min to disperse NPs in drilling fluid. To prepare Fe-XG NPs-based drilling fluid, Fe-XG was first mixed with water, and afterward, all components except barite were added and followed the same mixing procedure with 5 + 5 min. After adding barite, the same procedure of 5 + 5 min was followed. The main difference between the two fluids

is the addition of NPs. For iron oxide NPs without xanthan gum, the NPs were added in the end, while Fe-XG were added at the start, followed by other components.

Table 1. Composition of bentonite-based fluid.

Material	Base Fluid	Base Fluid + NPs
Water	350 mL	350 mL
Soda ash	4.8 g	4.8 g
Xanthan gum	0.71 g	0.71 g
Bentonite	10.04 g	10.04 g
Barite	183 g	183 g
Iron oxide NPs in water	-	0.05, 0.1, 0.2 g

Table 2. Composition of KCl-based fluid.

Material	Base Fluid	Base Fluid + NPs
Water	350 mL	350 mL
Soda ash	0.75 g	0.75 g
Xanthan gum	1.5 g	1.5 g
KCl	24.80 g	24.80 g
Barite	175 g	175 g
Iron oxide NPs in water	-	0.05, 0.1, 0.2 g

A similar procedure was followed to mix KCl-based fluids without and with NPs.

2.4. Drilling Fluid and NPs Characterization

Various characterization techniques were used to characterize NPs and drilling fluids with and without NPs. Details of the techniques are provided below.

2.4.1. Scanning Transmission Electron Microscopy (STEM)

A S-5500 STEM instrument (Hitachi, Krefeld, Germany) with a 30 kV accelerating voltage was used to obtain the STEM images of iron oxide NPs. Several drops of NPs solution were dropped on a Formvar carbon-coated copper grid to prepare TEM grids. It is crucial to wipe with Kimberly-Clark wipes after dropping the NPs solution to prevent further aggregation of NPs.

2.4.2. Microscale and Elemental Analysis

A Supra 35VP model scanning electron microscope (SEM, Zeiss, Oberkochen, Germany) was used to gain insights into the structural make-up and the presence of NPs in the mud cake from the fluid loss test. Additionally, images of the iron oxide NPs and Fe-XG were attained. Moreover, to quantify the percentage of different elements present in the structure and mapping, the elemental analysis was done with energy dispersive X-ray spectroscopy (EDS).

2.4.3. Dynamic Light Scattering (DLS) and Zeta Potential Measurements

A Zetasizer Nano-ZS instrument (Malvern, Worcestershire, UK) was used to measure the sizes and zeta potential of NPs. All the measurements were performed in aqueous solutions.

2.4.4. Viscosity

Viscosity parameters were measured using a model 900 viscometer (FANN, Houston, TX 77032, USA). Measurements were performed at 22 °C, 50 °C and 80 °C, and atmospheric pressure.

2.4.5. Mechanical Friction Measurement

The coefficient of friction was measured by using a CSM Tribometer (Anton Paar GmbH, Graz, Austria). The tests were conducted on a steel ball-plate surface filled with drilling fluid. The 13cr steel ball with a diameter of 6 mm was used. For all the tests normal load of 5 N was used that covered a 10 m distance with the rate of 3 cm/s. Measurements were performed at atmospheric pressure and room temperature. Repeat measurements were conducted to report the average value.

2.4.6. Fluid Loss Measurement

An American Petroleum Institute (API) filter press (FANN, Houston, TX 77032, USA) was used to measure the fluid loss at room temperature and 100 psi pressure. Filter paper with a diameter of 2.5 inches was used for the test. API standard, API Recommended Practice 13B-1 [40], was followed to perform the test.

2.4.7. Inductively Coupled Optical Atomic Emission Spectrometry (ICP-OES)

To measure the concentration of different ions, present in the filtrate obtained from the fluid loss test. ICP-OES analysis was performed before the analysis fluids were passed through a 0.2 µm syringe filter and diluted with 5% nitric acid.

2.4.8. Viscoelastic Measurement

Viscoelastic properties of the fluids were measured using a MCR 302 rheometer (Anton Paar GmbH, Graz, Austria). Amplitude sweep with a constant angular frequency of 10 rad/s and varying strain from 0.0005% to 1000% was performed.

3. Results and Discussion

3.1. Size Distribution of Iron Oxide and Fe-XG NPs

Figure 1a,b show the STEM and SEM images, respectively, of the NPs formed. It can be seen that particles have spherical morphology. Figure 2 show the size distribution of iron oxide NPs measured using STEM images. It can be seen in the figure that due to the absence of a stabilizing agent, particles formed have broad size distribution [41]. The average size of NPs formed by this method is 11 ± 2 nm.

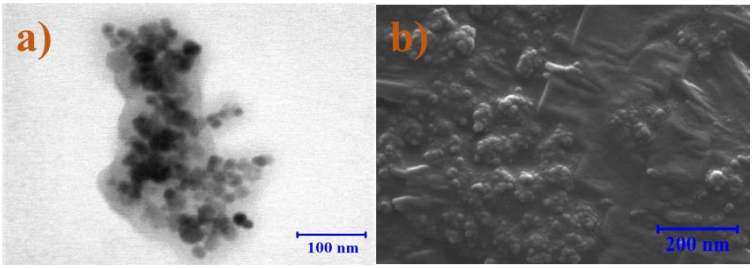

Figure 1. Iron oxide NPs formed by co-precipitation method: (**a**) STEM image; (**b**) SEM image.

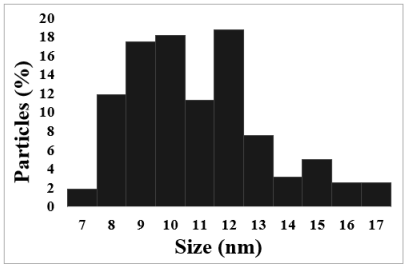

Figure 2. Size distribution of iron oxide NPs measured from STEM images.

Figure 3 shows the SEM images of Fe-XG, and it can be seen that the polymer is coated on the iron oxide NPs. Coating NPs with the polymer increases the particle size compared to the uncoated particles, as shown in Table 3.

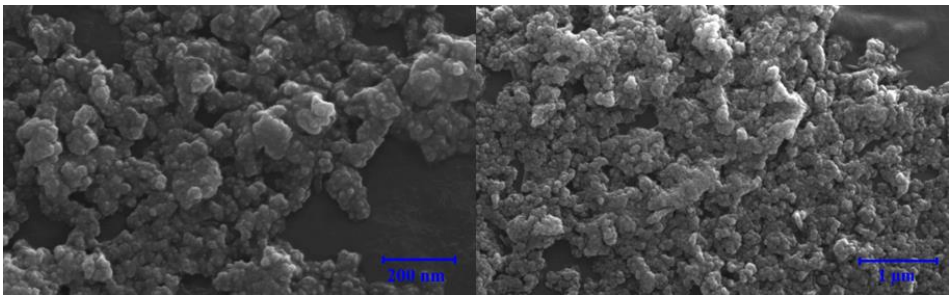

Figure 3. SEM images of Iron oxide NPs coated with xanthan gum (Fe-XG).

Table 3. Surface charges and sizes of NPs.

Material	Size (nm)	Zeta Potential (mV)
Iron oxide NPs at 25 °C	273.5 ± 5.95	−31.3 ± 0.27
Fe-XG NPs at 25 °C	487.60 ± 8.55	−39.23 ± 0.59
Iron oxide NPs at 50 °C	381.17 ± 19.58	−20.17 ± 0.23
Fe-XG NPs at 50 °C	673.57 ± 65.45	−34.37 ± 0.42

3.2. Hydrodynamic Size and Surface Charge of NPs

Table 3 shows the hydrodynamic size and surface charge of the iron oxide NPs and Fe-XG NPs. As shown in table, there is increase in size of NPs after coating of xanthan gum on their surface. Also, results show an increase in the size and decrease in zeta potential at higher temperatures. This indicates that NPs form aggregates at higher temperatures. Higher zeta potential values for Fe-XG indicate that polymer coating provides stability to the NPs and hinders the agglomeration and settling of NPs.

3.3. Rheological Parameters of the Drilling Fluids

3.3.1. Bentonite-Based Fluids

Shear stress values at different shear rates of bentonite-based drilling fluids are presented in Figure 4a–d. For base fluids and fluids with NPs, the shear stress values increase at high temperatures (i.e., 80 °C), especially at low shear rates. This is due to the inter-particle interaction of bentonite, which caused the flocculation of bentonite particles [42,43]. The clay particles agglomerate due to the face-to-face (FF) and edge-to-face (EF) associations [43,44]. A lower concentration (0.05 g) of NPs further increases the shear stress, as indicated in Figure 4a. A possible reason might be attachment of these NPs to edges of the clay platelets and with positively charged barium ions present in the drilling fluid. However, an increase in the NPs concentration (0.1 g) might cause repulsion between the negatively charged NPs and other negatively charged additives in the fluid system, which lowers the fluid's viscosity compared to the 0.05 g NPs as shown in Figure 4b.

Additionally, increasing the NPs concentration to 0.2 g might have caused agglomeration of NPs, which significantly increases the shear stress values, as indicated in Figure 4c. Although, coating of 0.2 g NPs with xanthan gum (Fe-XG) has decreased the shear stress values at a low shear rate, which indicates that polymer coating might have minimized the agglomeration of NPs and negatively charged polymer cause electrostatic repulsion between the negatively charged ions in the fluid system. Increase in zeta potential also indicates the stability of NPs with the polymer coating, see Table 3. In addition, there might be adsorption of polymer chains on the surface of bentonite prevented the

aggregation of bentonite at higher temperature [45]. Vryzas et al. [46] showed a similar behavior for the iron oxide NPs in the water-bentonite suspension. This study shows that bentonite forms a gel structure and aggregates at high temperature, due to the FF association of the platelets. Addition of NPs to these suspensions further increases the viscosity and yield stress due to aggregation of magnetic NPs owing to the high surface energies of the particles. However, the coating of NPs with citric acid minimizes the aggregation of NPs; our study shows a similar behavior with the coating of polymer on the NPs. Moreover, a decrease in the zeta potential of NPs at 50 °C, as indicated in the Table 3, also shows that high temperature reduces the stability of NPs, which causes the aggregation of the particles, especially at high concentration.

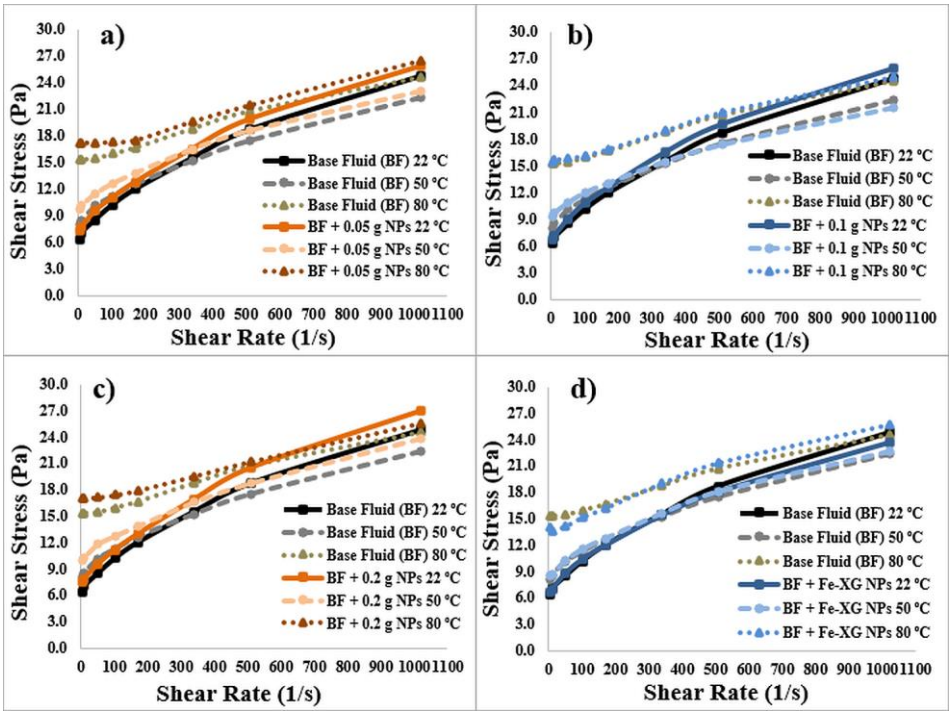

Figure 4. Iron oxide NPs effect on shear stress values of bentonite-based fluids at different shear rates and temperatures: (**a**) 0.05 g; (**b**) 0.1; (**c**) 0.2 g; (**d**) Fe-XG.

There is a decrease in apparent viscosity values with an increase in the shear rate for all the fluids, indicating the drilling fluid's shear-thinning behavior. Gel strength values (10 s and 10 min) are shown in Figure 5a,b for bentonite drilling fluids. A lower concentration of NPs (0.05 g) caused more increase in the base fluid's gel strength values than the 0.1 g NPs, especially for 10 min gel strength. This shows that NPs might get attached to the bentonite edges at low concentrations without causing the repulsion between the bentonite particles. However, increasing the NPs concentration, causing the deflocculation of the bentonite, precisely at 80 °C. At 80 °C, most of gel strength was attained after 10 s for all the fluids since gel strength did not change much when compared with gel strength measured at 10 min.

Gel strength with a higher concentration of NPs (0.2 g) and Fe-XG is also shown in Figure 5a,b. Increasing the NPs concentration raises the gel strength after 10 s and 10 min due to the agglomeration of NPs. However, coating the NPs surface with the xanthan gum again decreases the gel strength compared to 0.2 g NPs. This shows that the polymer surface on the NPs controls the agglomeration of NPs, and adsorption of polymer on bentonite prevents the gel formation, especially at 80 °C. Gel strength results for the bentonite-based fluid show high gel strength values that could efficiently hold the cutting and provide effective hole cleaning.

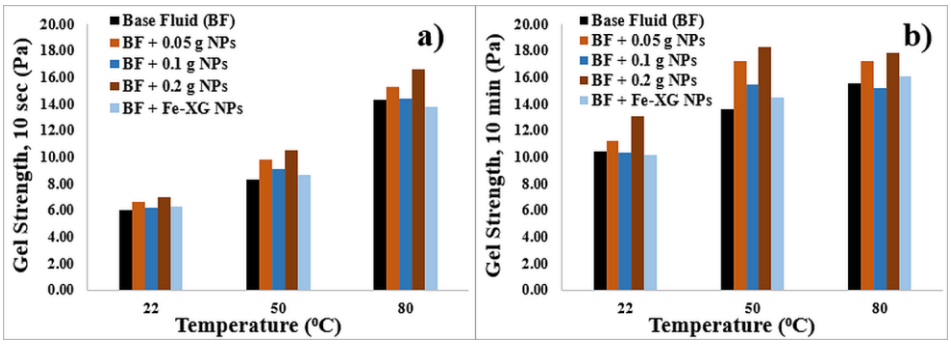

Figure 5. Gel strength of bentonite-based fluids: (**a**) 10 s gel strength; (**b**) 10 min gel strength.

3.3.2. KCL-Based Fluids

Figure 6a–d show the shear stress values at varying shear rates for the KCl-based fluids. High concentration of salt present in the fluids decreases the shear stress values at high temperature, as indicated in the figures. The high concentration of KCl salt makes the fluid system dispersive due to the suppression of the electric double layer.

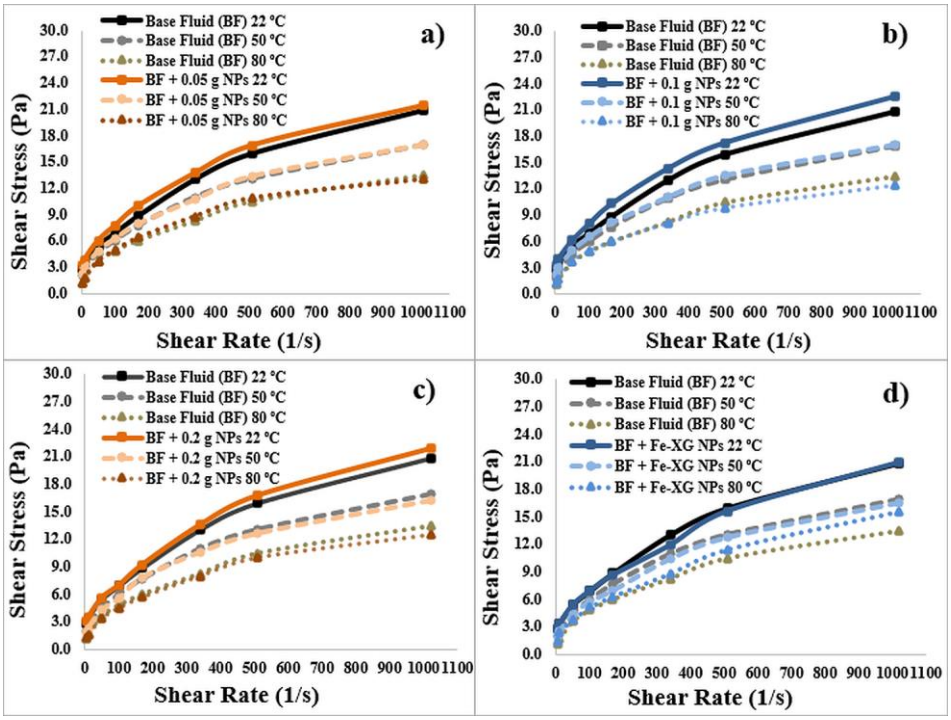

Figure 6. Iron oxide NPs effect on shear stress values of KCl-based fluids at different shear rates and temperatures: (**a**) 0.05 g; (**b**) 0.1; (**c**) 0.2 g; (**d**) Fe-XG.

Moreover, the addition of 0.05 g of NPs to the fluid system slightly increases the shear stress values at 22 °C and 50 °C, for instance increasing the shear stress values from 2.83 pa to 3.16 pa at 22 °C and 1.97 pa to 2.19 pa at 50 °C for a shear rate of 5.11 1/s. Similarly, for 0.1 g, there is a slight increase in shear stress values at 22 °C and 50 °C, as shown in Figure 6b. In case of 0.2 g, there is an increase in shear stress values at 22 °C. However, at 50 °C, addition of 0.2 g NPs lowers the shear stress value. For Fe-XG, there is not much change in the shear stress values as compared to the base fluid at 22 °C and 50 °C.

At 80 °C, uncoated NPs (0.05, 0.1, 0.2) do not have a significant effect on the shear stress values, in fact there is decrease in shear stress values especially at low shear rate. These results show that at high

temperature, NPs become unstable; this is also supported by the zeta potential measurements shown in Table 3. Polymer coating on the particles increases the shear stress at a higher shear rate for 80 °C compared to the uncoated and base fluid system that shows the improved stability of NPs with the polymer coating. Apparent viscosity in the case of KCl fluids also shows a decrease in values with an increase in the shear rate for all fluids.

Addition of NPs to the KCl drilling fluid slightly increases gel strength at 22 °C and 50 °C for both 10 s and 10 min, as shown in Figure 7a,b. However, at a higher temperature, NPs do not change the gel strength of base fluid. A decrease in zeta potential values of NPs indicates that at high-temperature NPs are agglomerated, which minimizes the interaction between NPs and KCl salt. Moreover, a high concentration of KCl present in the system forms weaker gel structures [47]. Additionally, Increasing the concentration and polymer coating decreases the gel strength compared to a base fluid at 22 °C, as shown in Figure 7. Fe-XG shows a minor increase in the gel strength at 80 °C, which might be due to the system's stability at higher temperatures due to polymer presence compared to the bare NPs.

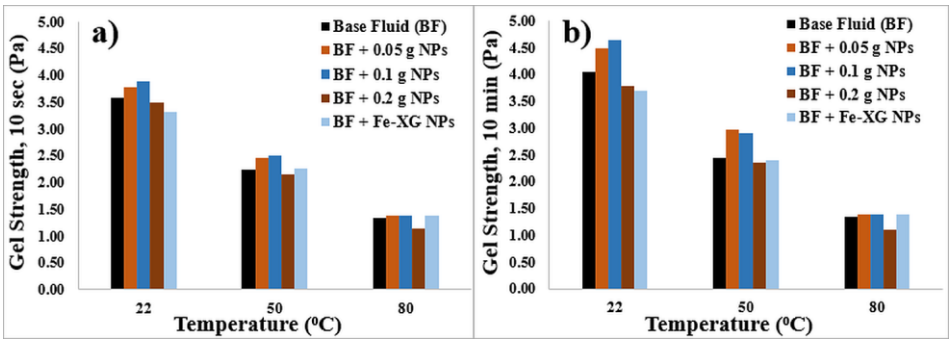

Figure 7. Gel strength values for KCl-based fluids: (**a**) Effect of temperature and NPs on 10 sec gel strength; (**b**) Effect of temperature and NPs on 10 min gel strength.

3.4. Viscoelasticity

Drilling fluids possess elastic and viscous properties [48,49]. Viscoelastic properties of the drilling fluids can provide further information about the drilling fluid's internal gel structure under dynamic loading. Storage and loss modules describe the energy stored and lost by the material when the shear is applied, respectively. Viscoelastic behavior of drilling fluids is presented in the next section for both types of fluid.

3.4.1. Bentonite-Based Fluids

Yield stress represents the stress where the deviation from the LVE region occurs and can be estimated from the shear stress and strain/time plot. Deviation of shear stress from linearity is taken as yield stress [50,51]. Flow points represent the point where storage and loss modules are equal. Table 4 shows the yield stress and flow point values for bentonite fluids. Figure 8a,b shows the storage and loss modulus for bentonite-based fluid and fluids with NPs.

Table 4. Yield stress and flow point for bentonite-based fluids.

Samples	Yield Stress (Pa)	Flow Point (Pa)
Base fluid (BF)	4.6	8.5
BF + 0.05 g NPs	5.6	9.3
BF + 0.1 g NPs	4.9	9.5
BF + 0.2 g NPs	5.2	8.9
BF + Fe-XG NPs	5.1	9.4

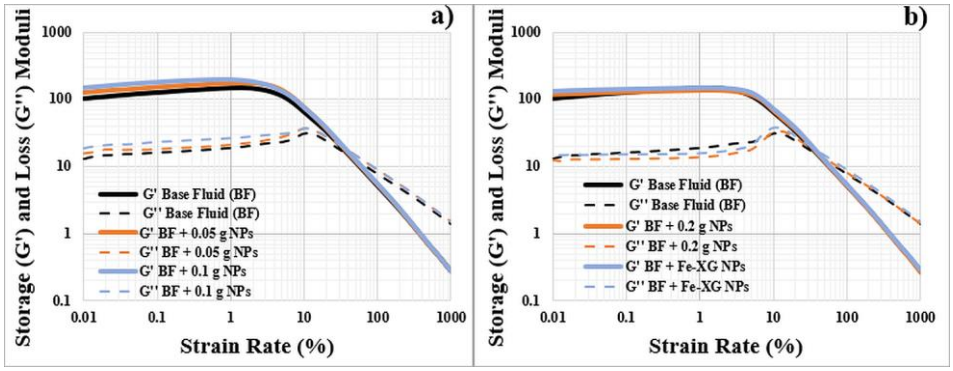

Figure 8. Storage and loss modulus for bentonite-based fluids: (**a**) Base fluid with low concentration of NPs; (**b**) Base fluid with high concentration of NPs and Fe-XG.

It can be seen that NPs slightly increases the yield stress values, especially for low concentration. However, increasing the concentration does not significantly alter the yield stress values. Moreover, in case of lower concentration NPs and Fe-XG, there is a slight delay in the flow point. This indicates that NPs provide structural strength to the fluid. However, raising the NPs concentration to 0.2 g slightly decreases the flow point compared to the low concentration.

3.4.2. KCL-Based Fluids

For KCl-based fluids, there is not much difference between the base fluids and fluids having NPs, as shown in Table 5 and Figure 9a,b. NPs addition decreases the flow point values compared to the base fluid in case of uncoated NPs. This shows that NPs addition slightly weakens the gel characteristics of KCl-based fluid. However, for Fe-XG, there is a slight increase in flow point, which shows the polymer's ability to improve the gel characteristics.

Table 5. Yield stress and flow point for KCl-based fluids.

Samples	Yield Stress (Pa)	Flow Point (Pa)
Base fluid (BF-1)	2.0	4.9
BF-1 + 0.05 g NPs	2.0	4.6
BF-1 + 0.1 g NPs	1.9	4.4
Base fluid (BF-2)	1.6	4.3
BF-2 + 0.2 g NPs	1.4	3.7
BF-2 + Fe-XG NPs	2.0	4.6

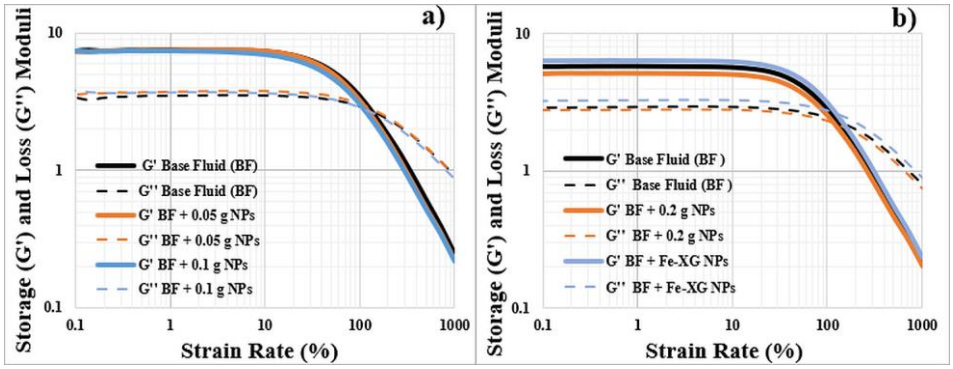

Figure 9. Storage and loss modulus for KCL-based fluid: (**a**) Base fluid with low concentration of NPs (**b**) Base fluid with high concentration of NPs and Fe-XG.

3.5. Mechanical Friction

Reducing the drilling fluid's mechanical friction is crucial to keep the torque and drag to a minimum during the drilling operation. Since minimizing the friction will allow drilling longer distances also, it makes the casing running operation smooth.

3.5.1. Bentonite-Based Fluids

Water-based drilling fluids with bentonite usually show higher values for mechanical friction. Therefore, it is beneficial to increase the lubricity of these fluids. As shown in Figure 10a, NPs have reduced the coefficient of friction of base fluids. NPs with 0.1 g concentration shows the most reduction in friction values. However, a higher concentration of NPs increases friction. The possible reason might be the agglomeration of NPs at higher concentrations.

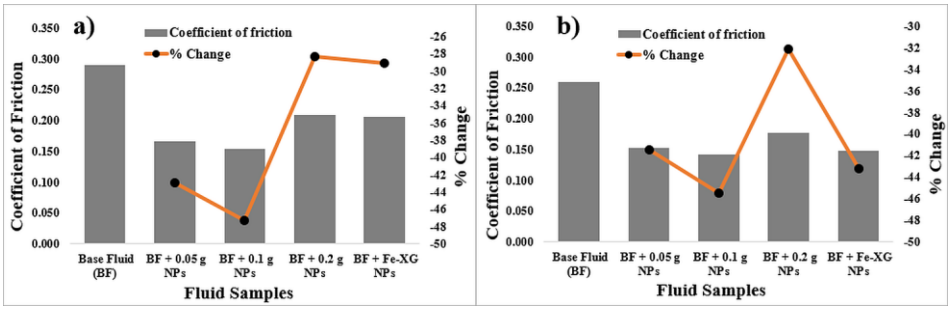

Figure 10. Friction values of: (**a**) Bentonite-based fluids with NPs; (**b**) KCl-based fluids with NPs.

3.5.2. KCl-Based Fluids

Since KCl-based fluids do not have bentonite present in them, they show low mechanical friction values compared to bentonite-based fluids, as indicated in Figure 10b. NPs also decrease the coefficient of friction in case of these fluid systems. In this case, also, 0.1 g NPs showed the most reduction in friction values. However, all the other concentrations of NPs still provide a significant reduction in friction. These results for both water-based fluids show that NPs can provide lubricating properties to the drilling fluids. NPs form a lubricating film around the micro-sized material's harsh surfaces and behave like a fluid in the system.

3.6. Effect of NPs on the Fluid Loss

Since the quality of drilling fluid is dependent on its performance with respect to controlling the filtrate loss to the formation, it is crucial to minimize the fluid loss. The additives and solid particles that form the filter cake are vital in controlling the fluid loss.

3.6.1. Bentonite-Based Fluids

Figure 11a shows the fluid loss results for the bentonite-based fluids with and without NPs. As shown in the figure, NPs have reduced the fluid loss for the base fluids. NPs with 0.05 g, 0.1 g and 0.2 g concentration reduced the fluid loss by 20%, 13% and 19% respectively. NPs coated with xanthan gum reduces fluid loss by 16%. The results indicate that NPs with different concentrations show a similar reduction in fluid loss, with low concentration showing the most reduction. This might be due to the even distribution of NPs on filter cake and the fluid's stability under pressure. However, 0.2 g NPs show almost the same amount of reduction due to filling the micropores in the filter cake by the NPs.

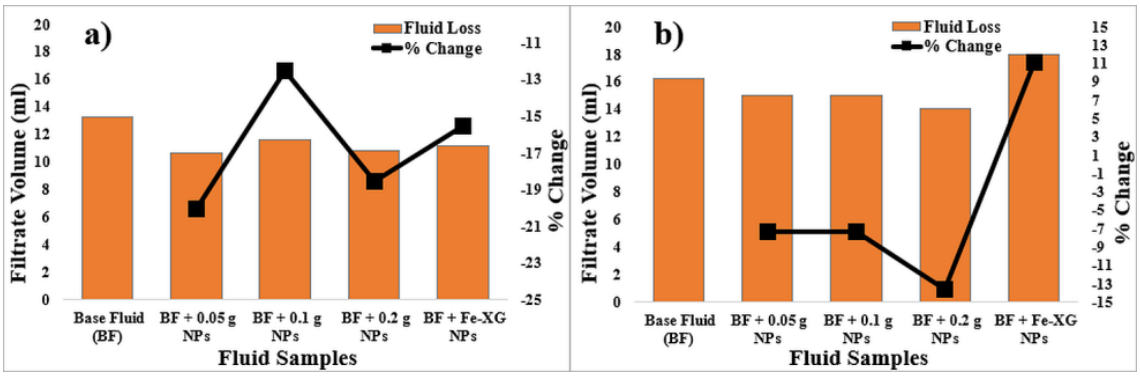

Figure 11. Filtrate volume after fluid loss test for: (**a**) Bentonite-based fluids with NPs; (**b**) KCl-based fluids with NPs.

3.6.2. KCL-Based Fluids

For the KCl fluids, a higher concentration (0.2 g) of NPs showed the highest reduction of 14% in fluid loss. Fluids with 0.05 g and 0.1 g concentration NPs reduce fluid loss by 7%, as shown in Figure 11b. However, NPs coated with xanthan gum increases fluid loss. This might be due to the large size of the particles are not able to fill the pores compared to the uncoated particles. It can be seen that KCl based fluid showed higher values for fluid loss due to the absence of bentonite in the system. Moreover, lower apparent viscosity of the KCl-based fluids than the bentonite fluids also contributed to higher values of fluid loss.

3.7. Microscale Analysis of the Filter Cake

3.7.1. Bentonite-Based Fluids

SEM images for the cake formed by bentonite-based fluid are shown in the Figure 12. It can be seen in Figure 12a,b that the cake formed by the base fluid is not compact and there are voids in the cake structure. Addition of NPs results in a less porous and compact structure formation for the base fluid (see Figure 12c,d for iron oxide NPs and Figure 12e,f for Fe-XG NPs). Other studies also report similar results with bentonite-based drilling fluids [30,35,52].

The possible reason for the reduction in fluid loss is the filling of voids in the cake structure by the NPs, as indicated in Figures 13 and 14. However, as indicated in figures for both bare NPs and Fe-XG that there is an agglomeration of NPs, which might hinder the further reduction in the fluid loss due to less particle packing. EDS spectrum of the area pointed by the arrow shows higher concentration of Fe, indicating the presence of iron oxide NPs in the cake.

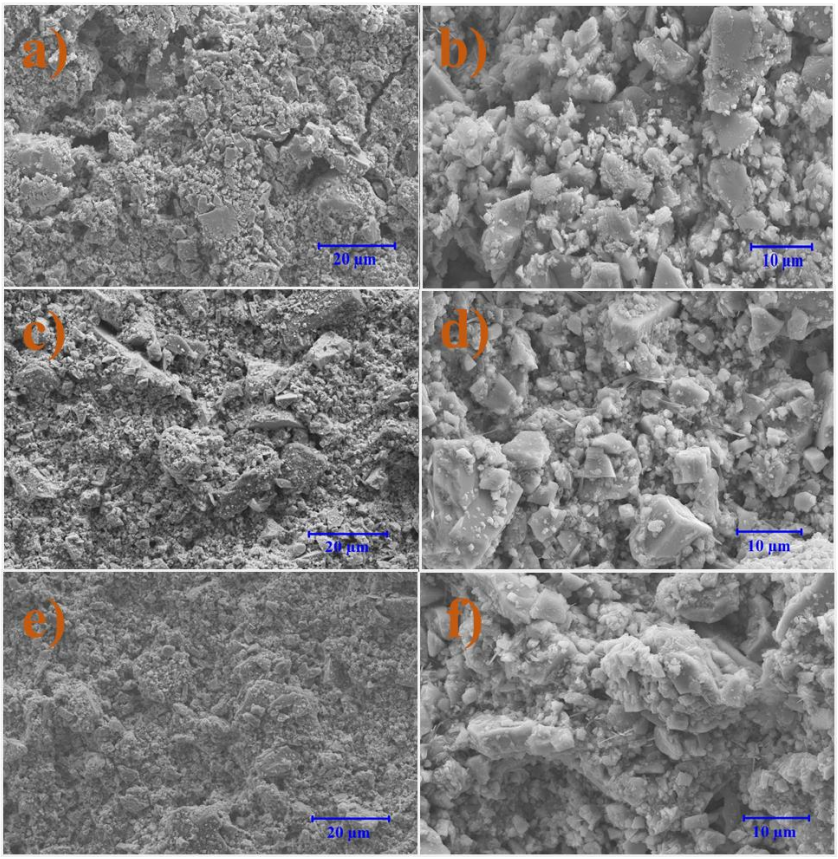

Figure 12. SEM images of filter cake of Bentonite-based fluids: (**a**,**b**) Filter cake for base fluids; (**c**,**d**) Filter cake for base fluids with Iron oxide NPs; (**e**,**f**) Filter cake for base fluids with Fe-XG NPs.

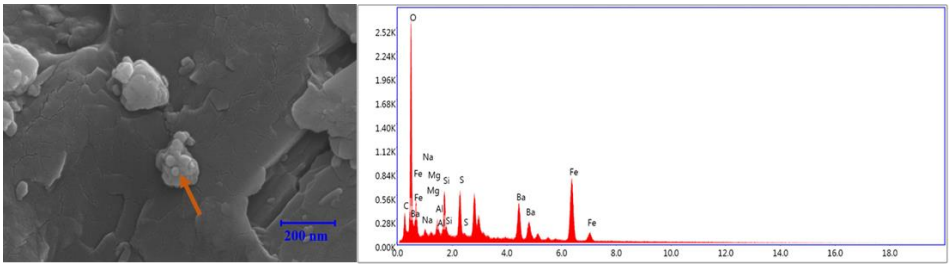

Figure 13. Presence of NPs in the mud cake for bentonite fluids with iron oxide NPs (EDS spectrum shows the analysis done on the area indicated by the arrow).

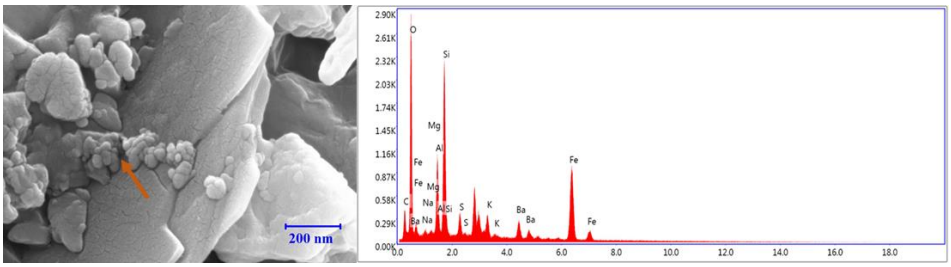

Figure 14. Presence of NPs in the mud cake for bentonite fluids with Fe-XG NPs (EDS spectrum shows the analysis done on the area pointed by the arrow).

3.7.2. KCl-Based Fluids

Figure 15a–f show the SEM images for the KCl-based fluid and base fluids with NPs. NPs can produce a less porous structure by filling the voids in the structure of mud cake. However, as indicated in figures, voids are still present in the cake structure, where they are responsible for higher fluid loss values.

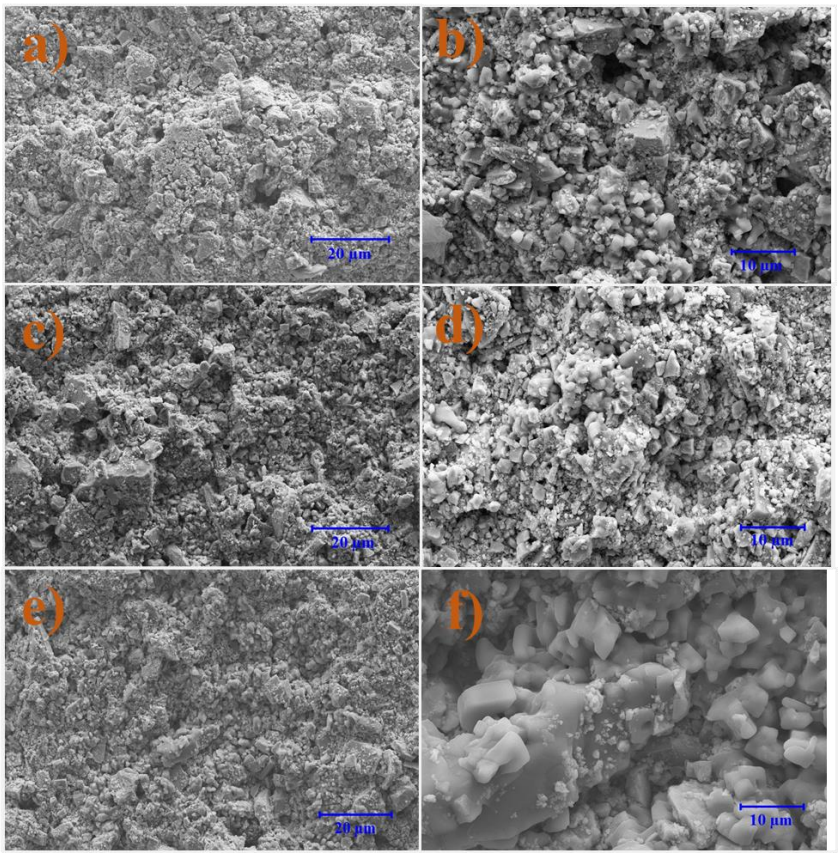

Figure 15. SEM images of filter cake KCl-based fluids: (**a**,**b**) Filter cake for base fluids; (**c**,**d**) Filter cake for base fluids with Iron oxide NPs; (**e**,**f**) Filter cake for base fluids with Fe-XG NPs.

In case of the sample with iron oxide NPs, closer observation of the mud cake structure indicates that for bare NPs, there is a filling of the voids between the micro-sized particles by the NPs as shown in Figure 16. Also, NPs interacted with the salt surface leading to a compact structure compared to microparticles.

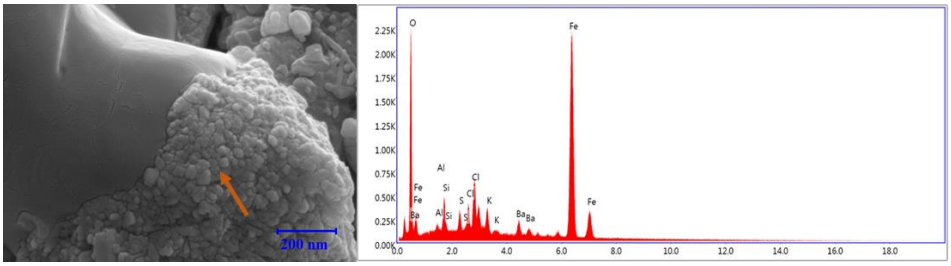

Figure 16. Presence of NPs in the mud cake for KCl fluids with Iron oxide NPs (EDS spectrum shows the analysis done on the area pointed by the arrow).

However, for Fe-XG, the higher values for the fluid loss might be due to NPs got adsorbed on the salt surface and not being able to fill the voids in the cake's structure. Also, large size of the particles did not create compact cake structure, as shown in Figure 17. Moreover, dissociation of salt induces flocculation by reducing the polymer interaction with the other additives and creating voids in the structure.

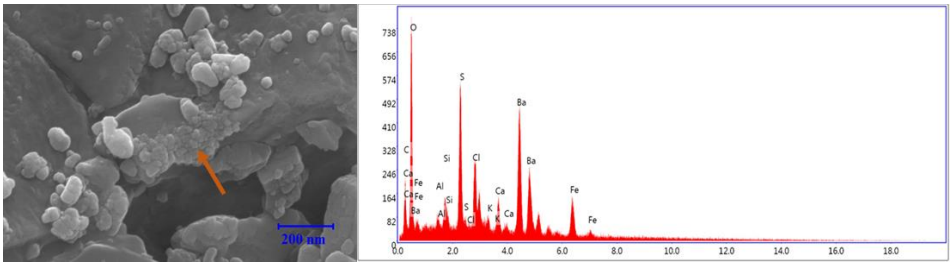

Figure 17. Presence of NPs in the mud cake for KCl fluids with Fe-XG NPs (EDS spectrum shows the analysis done on the area pointed by the arrow).

3.8. EDS Analysis

3.8.1. Bentonite-Based Fluids

The main elements present in the filter cake for the bentonite-based system are sodium, oxygen, barium, sulphur and silicon. Small amounts of magnesium, calcium, aluminum, and strontium are present in the cake formed after the fluid loss test. Figures 18a–c and 19a–c show the presence of iron in the cake structures formed by bentonite-based fluids and KCl-based fluids, respectively. Figure 18b indicates that the iron oxide NPs are distributed in the cake structure, and the iron (Fe) amount also increases compared to the base fluid. However, in case of Fe-XG NPs, as seen in Figure 18c, there is no uniform distribution of NPs. This indicates that the Fe-XG particles remain dispersed in the fluid without contributing to cake formation. Fe content is also lowered in this case compared to the samples with uncoated NPs due to xanthan gum's coating on the surface of the particles.

3.8.2. KCl-Based Fluids

In case of KCl fluids, there is a higher concentration of potassium and chlorine present in the cake structure. Moreover, a lower amount of sodium is present due to the absence of bentonite.

Similarly, in the case of KCl fluids, the iron oxide NPs contributed to cake formation as Fe content increase in case of samples with NPs, see Figure 19b. However, NPs filled few voids in the structure, creating a less compact structure leading to lower fluid loss reduction.

Additionally, mapping results indicate that for Fe-XG, NPs were not uniformly distributed in the cake structure. Also, NPs do not fill the voids in the cake structure, which leads to an increase in the fluid loss values, as shown in Figure 19c.

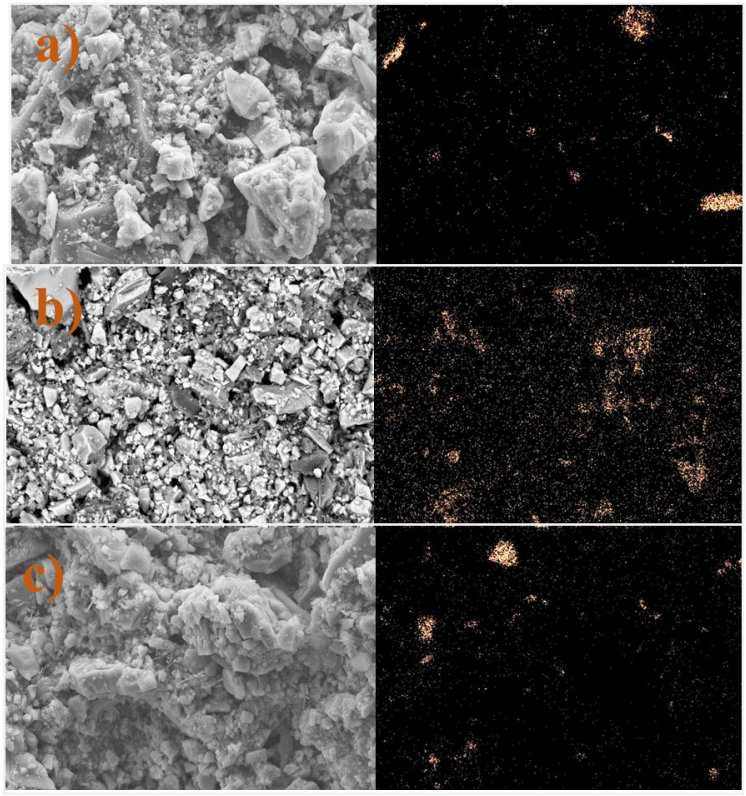

Figure 18. Elemental analysis of filter cake for bentonite-based fluids: (**a**) Base fluid; (**b**) Base fluid with NPs; (**c**) Base fluid with Fe-XG NPs.

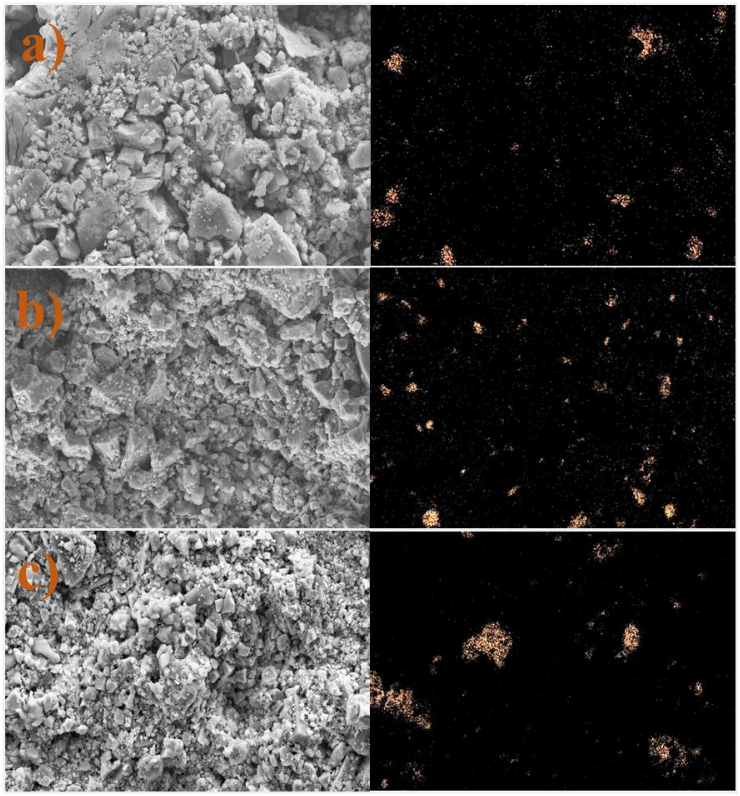

Figure 19. Elemental analysis of filter cake for KCl-based fluids: (**a**) Base fluid; (**b**) Base fluid with NPs; (**c**) Base fluid with Fe-XG NPs.

3.9. Elemental Analysis of Filtrate

Element analysis results are shown in Tables 6 and 7. In case of low concentrations of NPs, there was no iron detected in the filtrate. However, increasing the concentration shows that iron was present in the filtrate. This shows that most of NPs are deposited on a cake or stayed in the drilling fluid at a lower concentration. Even at higher concentrations, there is small amount of iron particles present in the filtrate. Most of the particles stayed on the cake and in the drilling fluid. A high concentration of sodium was detected in the bentonite-based fluids. In comparison, KCl-based fluids showed a higher concentration of potassium cations present in the filtrate. Most of the barite stayed in the cake as low barium and sulfate concentrations were detected, as shown in the tables.

Table 6. Elements from the filtrate loss for bentonite-based fluids.

Elements	Base Fluid	Base Fluid + 0.05 g NPs	Base Fluid + 0.2 g NPs	Base Fluid + Fe-XG
Barium, Ba (mg/L)	0.31	0.27	0.27	0.30
Calcium Ca (mg/L)	0.7	1.0	0.5	0.6
Copper Cu (mg/L)	0.7	0.91	0.6	0.6
Iron Fe (mg/L)	n.d.	n.d.	0.09	<0.06
Potassium K (mg/L)	237	108	123	35
Magnesium Mg (mg/L)	2.2	2.1	2.3	2.4
Sodium Na (mg/L)	5906	5579	5460	5370
Silicon Si (mg/L)	5.6	5.6	4.5	5.3
Strontium Sr (mg/L)	0.9	1.3	0.5	0.3
Aluminium Al (mg/L)	1.4	<0.5	2.0	2.3

Table 7. Elements from the filtrate loss for KCl-based fluids.

Elements	Base Fluid	Base Fluid + 0.05 g NPs	Base Fluid + 0.2 g NPs	Base Fluid + Fe-XG
Barium, Ba (mg/L)	1.8	1.2	1.4	1.6
Calcium Ca (mg/L)	<3	<3	2.1	3.7
Copper Cu (mg/L)	1.9	1.5	1.5	1.4
Iron Fe (mg/L)	n.d.	n.d.	<0.3	<0.3
Potassium K (mg/L)	36,144	35,564	33,400	32,700
Magnesium Mg (mg/L)	4	4	4	3.2
Sodium Na (mg/L)	894	826	820	850
Silicon Si (mg/L)	<3	<3	2.4	2.6
Strontium Sr (mg/L)	9.3	8.6	8.3	8.3
Aluminium Al (mg/L)	<5	<5	<5	<5

3.10. Magnetic Recovery

Magnetic recovery of the NPs from the drilling fluids was done by using a strong magnet. It can be seen that NPs can be recovered from the fluid system. These recovered particles were analyzed using SEM, as shown in Figures 20 and 21 for bentonite and KCl-based fluids, respectively. As seen from the figures, NPs interacted with the other components of the drilling fluids. For both bentonite and KCl fluids high concentration of barium indicated that NPs interacted with the barium. A small amount of sodium and magnesium was also present in bentonite-based fluids indicating the interaction of particles with bentonite. Moreover, the EDS spectrum shows small amounts of potassium and chlorine for the KCl-based fluids.

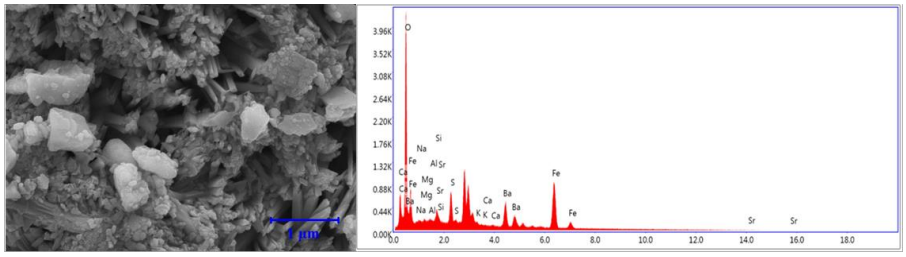

Figure 20. SEM image and EDS spectrum of recovered particles for bentonite-based fluids.

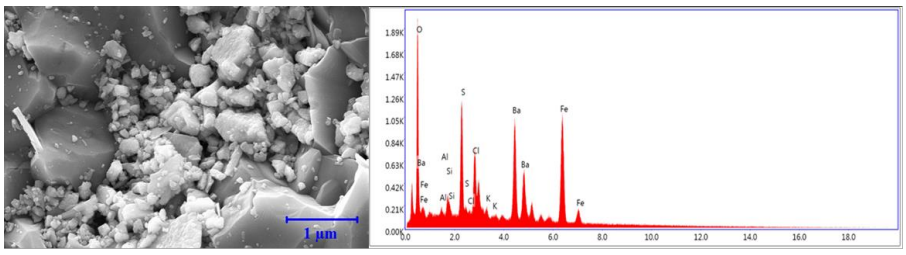

Figure 21. SEM image and EDS spectrum of recovered particles for KCl-based fluid.

4. Conclusions

In this experimental study, iron oxide NPs and Fe-XG NPs effect on two types of water-based drilling fluids (bentonite-based fluids and KCl-based fluids) was studied. The main findings of the study are summarized below:

- Results indicate that NPs can modify the rheological parameters of bentonite-based fluids. NPs increases the viscosity and gel strength of the bentonite-based fluids owing to the agglomeration of magnetic NPs.
- A polymer coating on the NPs slightly reduces the gel strength values at high temperature for bentonite-based fluids.
- Small concentration of NPs was sufficient to reduce the coefficient of friction and fluid loss values of the bentonite-based fluids. NPs with 0.019 wt% (0.1 g) and 0.0095 wt% (0.05 g) reduces the coefficient of friction and fluid loss by 47% and 20%, respectively.
- Fe-XG NPs also reduces the coefficient of friction by 29%, while fluid loss values were reduced by 16% for bentonite-based fluids.
- Filter cake analysis shows that NPs filled the spaces in the structure of the cake and uniform distribution of particles kept the fluid loss values to a minimum compared to the base fluid.
- In addition, elemental analysis shows the even distribution of the NPs throughout the structure of the filter cake.
- In the case of KCl-based fluids, the addition of NPs has a slight impact on rheological parameters owing to the lesser stability of the fluid system due to presence of high salt concentration.

- In case of coefficient of friction and fluid loss, NPs do provide improvements. Addition of 0.038 (0.2 g) wt%, and 0.019 wt% (0.1 g) of NPs reduces fluid loss and friction by 14% and 45%, respectively. However, Fe-XG NPs increase the fluid loss value by 11%.
- Microscale analysis of the cake shows that NPs do interact with the salt and reduce the cake's permeability by forming compact structures.
- Fe-XG NPs increases the fluid loss values due to an increase in size and adsorption of polymer on the salt surface, creating voids in the cake structure.
- This work also shows that magnetic recovery of NPs also provides further information regarding the interaction of NPs with other additives in the drilling fluid system.
- This study shows that low concentration of NPs is sufficient to improve the properties of drilling fluids. Also, NPs can reduce the fluid loss values and friction values of KCl-based fluids without affecting the rheological parameters.

Author Contributions: Conceptualization, methodology, investigation, formal analysis, writing—original draft, writing—review & editing, M.A.A.A.; conceptualization, supervision, project administration, funding acquisition, writing—review & editing, M.B.; conceptualization, supervision, project administration, funding acquisition, S.B.; formal analysis, investigation, validation, resources, M.W.M. All authors have read and agreed to the published version of the manuscript.

Funding: This research was funded by Norwegian Ministry of Education and Research, project number 8050-IN11398 and Norwegian micro- and Nano-Fabrication facility, NorFab project number 245963.

Acknowledgments: Authors would like to thank Kjell Kåre Fjelde for contributing in reviewing the paper and Muhammad Bilal for helping with DLS and zeta potential measurements.

Conflicts of Interest: The authors declare no conflict of interest.

References

1. Bourgoyne, A.T.; Millhelm, K.K.; Chenevert, M.E.; Young, F.S., Jr. *Applied Drilling Engineering*; Textbook Series Vol. 2; Society of Petroleum Engineering: Richardson, TX, USA, 1986.
2. Caenn, R.; Darley, H.C.H.; Gray, G.R. Introduction to Drilling Fluids. In *Composition and Properties of Drilling and Completion Fluids*; Gulf Professional Publishing: Houston, TX, USA, 2017.
3. He, S.; Liang, L.; Zeng, Y.; Ding, Y.; Lin, Y.; Liu, X. The influence of water-based drilling fluid on mechanical property of shale and the wellbore stability. *Petroleum* **2016**, *2*, 61–66. [CrossRef]
4. Ewy, R.T.; Morton, E.K. Wellbore-Stability Performance of Water-Based Mud Additives. *SPE Drill. Complet.* **2009**, *24*, 390–397. [CrossRef]
5. Jones, T.G.J.; Hughes, T.L. Drilling Fluid Suspensions. *Adv. Chem. Ser.* **1996**, *251*. [CrossRef]
6. Al-Yasiri, M.; Awad, A.; Pervaiz, S.; Wen, D. Influence of silica nanoparticles on the functionality of water-based drilling fluids. *J. Pet. Sci. Eng.* **2019**, *179*, 504–512. [CrossRef]
7. Agarwal, S.; Phuoc, T.X.; Soong, Y.; Martello, D.; Gupta, R.K. Nanoparticle-stabilised invert emulsion drilling fluids for deep-hole drilling of oil and gas. *Can. J. Chem. Eng.* **2013**, *91*, 1641–1649. [CrossRef]
8. Fink, J. *Petroleum Engineer's Guide to Oil Field Chemicals and Fluids*; Gulf Professional Publishing: Houston, TX, USA, 2012. [CrossRef]
9. Abdo, J.; Haneef, M.D. Nano-Enhanced Drilling Fluids: Pioneering Approach to Overcome Uncompromising Drilling Problems. *J. Energy Resour. Technol.* **2012**, *134*, 014501. [CrossRef]
10. Abdo, J.; AL-Sharji, H.; Hassan, E. Effects of nano-sepiolite on rheological properties and filtration loss of water-based drilling fluids. *Surf. Interface Anal.* **2016**, *48*, 522–526. [CrossRef]
11. Ghanbari, S.; Kazemzadeh, E.; Soleymani, M.; Naderifar, A. A facile method for synthesis and dispersion of silica nanoparticles in water-based drilling fluid. *Colloid Polym. Sci.* **2016**, *294*, 381–388. [CrossRef]
12. Jain, R.; Mahto, V.; Sharma, V.P. Evaluation of polyacrylamide-grafted-polyethylene glycol/silica nanocomposite as potential additive in water based drilling mud for reactive shale formation. *J. Nat. Gas Sci. Eng.* **2015**, *26*, 526–537. [CrossRef]
13. Katende, A.; Boyou, N.V.; Ismail, I.; Chung, D.Z.; Sagala, F.; Hussein, N.; Ismail, M.S. Improving the performance of oil based mud and water based mud in a high temperature hole using nanosilica nanoparticles. *Colloids Surf. A Physicochem. Eng. Asp.* **2019**, *577*, 645–673. [CrossRef]

14. Sadeghalvaad, M.; Sabbaghi, S. The effect of the TiO_2/polyacrylamide nanocomposite on water-based drilling fluid properties. *Powder Technol.* **2015**, *272*, 113–119. [CrossRef]
15. Alvi, M.A.A.; Belayneh, M.; Saasen, A.; Fjelde, K.K.; Aadnøy, B.S. Effect of MWCNT and MWCNT functionalized -OH and -COOH nanoparticles in laboratory water based drilling fluid. In Proceedings of the ASME 37th International Conference on Ocean, Offshore & Arctic Engineering (OMAE), Madrid, Spain, 17–22 June 2018. [CrossRef]
16. Aftab, A.; Ismail, A.R.; Khokhar, S.; Ibupoto, Z.H. Novel zinc oxide nanoparticles deposited acrylamide composite used for enhancing the performance of water-based drilling fluids at elevated temperature conditions. *J. Pet. Sci. Eng.* **2016**, *146*, 1142–1157. [CrossRef]
17. Halali, M.A.; Ghotbi, C.; Tahmasbi, K.; Ghazanfari, M.H. The Role of Carbon Nanotubes in Improving Thermal Stability of Polymeric Fluids: Experimental and Modeling. *Ind. Eng. Chem. Res.* **2016**, *55*, 7514–7534. [CrossRef]
18. Song, K.; Wu, Q.; Li, M.C.; Wojtanowicz, A.K.; Dong, L.; Zhang, X.; Ren, S.; Lei, T. Performance of low solid bentonite drilling fluids modified by cellulose nanoparticles. *J. Nat. Gas Sci. Eng.* **2016**, *34*, 1403–1411. [CrossRef]
19. Song, K.; Wu, Q.; Li, M.; Ren, S.; Dong, L.; Zhang, X.; Lei, T.; Kojima, Y. Water-based bentonite drilling fluids modified by novel biopolymer for minimizing fluid loss and formation damage. *Colloids Surf. A Physicochem. Eng. Asp.* **2016**, *507*, 58–66. [CrossRef]
20. William, J.K.M.; Ponmani, S.; Samuel, R.; Nagarajan, R.; Sangwai, J.S. Effect of CuO and ZnO nanofluids in xanthan gum on thermal, electrical and high pressure rheology of water-based drilling fluids. *J. Pet. Sci. Eng.* **2014**, *117*, 15–27. [CrossRef]
21. Mao, H.; Qiu, Z.; Shen, Z.; Huang, W. Hydrophobic associated polymer based silica nanoparticles composite with core-shell structure as a filtrate reducer for drilling fluid at utra-high temperature. *J. Pet. Sci. Eng.* **2015**, *129*, 1–14. [CrossRef]
22. Taha, N.M.; Lee, S. Nano Graphene Application Improving Drilling Fluids Performance. In Proceedings of the International Petroleum Technology Conference, Doha, Qatar, 6–9 December 2015. [CrossRef]
23. Fazelabdolabadi, B.; Khodadadi, A.A.; Sedaghatzadeh, M. Thermal and rheological properties improvement of drilling fluids using functionalized carbon nanotubes. *Appl. Nanosci.* **2015**, *5*, 651–659. [CrossRef]
24. Sadegh Hassani, S.; Amrollahi, A.; Rashidi, A.; Soleymani, M.; Rayatdoost, S. The effect of nanoparticles on the heat transfer properties of drilling fluids. *J. Pet. Sci. Eng.* **2016**, *146*, 183–190. [CrossRef]
25. Kang, Y.; She, J.; Zhang, H.; You, L.; Song, M. Strengthening shale wellbore with silica nanoparticles drilling fluid. *Petroleum* **2016**, *2*, 189–195. [CrossRef]
26. Nwaoji, C.O.; Hareland, G.; Husein, M.; Nygaard, R.; Zakaria, M.F. Wellbore strengthening- nano-particle drilling fluid experimental design using hydraulic fracture apparatus. In Proceedings of the SPE/IADC Drilling Conference, Amsterdam, The Netherlands, 5–7 March 2013. [CrossRef]
27. Sharma, M.M.; Zhang, R.; Chenevert, M.E.; Ji, L.; Guo, Q.; Friedheim, J. A new family of nanoparticle based drilling fluids. In Proceedings of the SPE Annual Technical Conference and Exhibition, San Antonio, TX, USA, 8–10 October 2012. [CrossRef]
28. Aramendiz, J.; Imqam, A. Water-based drilling fluid formulation using silica and graphene nanoparticles for unconventional shale applications. *J. Pet. Sci. Eng.* **2019**, *179*, 742–749. [CrossRef]
29. Jung, Y.; Barry, M.; Lee, J.-K.; Tran, P.; Soong, Y.; Martello, D.; Chyu, M. Effect of nanoparticle-additives on the rheological properties of clay-based fluids at high temperature and high pressure. In Proceedings of the AADE National Technical Conference and Exhibition, Houston, TX, USA, 12–14 April 2011; pp. 1–4.
30. Barry, M.M.; Jung, Y.; Lee, J.K.; Phuoc, T.X.; Chyu, M.K. Fluid filtration and rheological properties of nanoparticle additive and intercalated clay hybrid bentonite drilling fluids. *J. Pet. Sci. Eng.* **2015**, *127*, 338–346. [CrossRef]
31. Mahmoud, O.; Nasr-El-Din, H.A.; Vryzas, Z.; Kelessidis, V.C. Characterization of filter cake generated by nanoparticle-based drilling fluid for HP/HT applications. In Proceedings of the SPE International Conference on Oilfield Chemistry, Montgomery, TX, USA, 3–5 April 2017. [CrossRef]
32. Vryzas, Z.; Mahmoud, O.; Nasr-El-Din, H.; Zaspalis, V.; Kelessidis, V.C. Incorporation of Fe_3O_4 nanoparticles as drilling fluid additives for improved drilling operations. In Proceedings of the ASME 35th International Conference on Ocean, Offshore & Arctic Engineering (OMAE), Busan, Korea, 19–24 June 2016. [CrossRef]
33. Vryzas, Z.; Zaspalis, V.; Nalbantian, L.; Mahmoud, O.; Nasr-El-Din, H.A.; Kelessidis, V.C. A comprehensive approach for the development of new iron oxide nanoparticles giving smart drilling fluids with superior properties for HP/HT applications. In Proceedings of the International Petroleum Technology Conference, Bangkok, Thailand, 14–16 November 2016. [CrossRef]

34. Mahmoud, O.; Nasr-El-Din, H.A.; Vryzas, Z.; Kelessidis, V.C. Effect of ferric oxide nanoparticles on the properties of filter cake formed by calcium bentonite-based drilling muds. *SPE Drill. Complet.* **2018**, *33*. [CrossRef]
35. Mahmoud, O.; Nasr-El-din, H.A.; Vryzas, Z.; Kelessidis, V.C. Using ferric oxide and silica nanoparticles to develop modified calcium bentonite drilling fluids. *SPE Drill. Complet.* **2018**, *33*. [CrossRef]
36. Alvi, M.A.A.; Belayneh, M.; Saasen, A.; AadnØy, B.S. The effect of micro-sized boron nitride BN and iron trioxide Fe_2O_3 nanoparticles on the properties of laboratory bentonite drilling fluid. In Proceedings of the SPE Norway One Day Seminar, Bergen, Norway, 18 April 2018. [CrossRef]
37. Shi, X.; Wang, L.; Guo, J.; Su, Q.; Zhuo, X. Effects of inhibitor KCl on shale expansibility and mechanical properties. *Petroleum* **2019**, *5*, 407–412. [CrossRef]
38. Puddu, M.; Paunescu, D.; Stark, W.J.; Grass, R.N. Magnetically recoverable, thermostable, hydrophobic DNA/silica encapsulates and their application as invisible oil tags. *ACS Nano* **2014**, *8*, 2677–2685. [CrossRef]
39. Torsvik, A.; Myrseth, V.; Opedal, N.; Lund, B.; Saasen, A.; Ytrehus, J.D. Rheological comparison of bentonite based and KCl/polymer based drilling fluids. *Annu. Trans. Nord. Rheol. Soc.* **2014**, *22*, 219–224.
40. API. *Recommended Practice for Field Testing Water-Based Drilling Fluids*; 13B-1 APIRP; API: Washington, DC, USA, 2009.
41. Sharma, A.; Foppen, J.W.; Banerjee, A.; Slimani, S.; Bachhar, N.; Peddis, D.; Bandyopadhyay, S. Magnetic Nanoparticles to Unique DNA Tracers—Effect of Functionalization on Physico-Chemical Properties. *Nanoscale Res. Lett.* **2020**. [CrossRef]
42. Darley, H.C.H.; Gray, G.R. *Composition and Properties of Drilling and Completion Fluids*; Gulf Professional Publishing: Houston, TX, USA, 1988.
43. Vryzas, Z.; Kelessidis, V.C.; Nalbantian, L.; Zaspalis, V.; Gerogiorgis, D.I.; Wubulikasimu, Y. Effect of temperature on the rheological properties of neat aqueous Wyoming sodium bentonite dispersions. *Appl. Clay Sci.* **2017**, *136*, 26–36. [CrossRef]
44. Mouzon, J.; Bhuiyan, I.U.; Hedlund, J. The structure of montmorillonite gels revealed by sequential cryo-XHR-SEM imaging. *J. Colloid Interface Sci.* **2016**, *465*, 58–66. [CrossRef]
45. Ahmad, H.M.; Kamal, M.S.; Al-Harthi, M.A. Rheological and filtration properties of clay-polymer systems: Impact of polymer structure. *Appl. Clay Sci.* **2018**, *160*, 226–237. [CrossRef]
46. Vryzas, Z.; Nalbandian, L.; Zaspalis, V.T.; Kelessidis, V.C. How different nanoparticles affect the rheological properties of aqueous Wyoming sodium bentonite suspensions. *J. Pet. Sci. Eng.* **2019**, *173*, 941–954. [CrossRef]
47. Chang, W.Z.; Leong, Y.K. Ageing and collapse of bentonite gels—Effects of Li, Na, K and Cs ions. *Rheologica Acta* **2014**, *53*, 109–122. [CrossRef]
48. Bui, B.; Saasen, A.; Maxey, J.; Ozbayoglu, M. Viscoelastic Properties of Oil-Based Drilling Fluids. *Annu. Trans. Nord. Rheol. Soc.* **2012**, *20*, 33–47.
49. Saasen, A.; Liu, D.; Marken, C.D. Prediction of barite sag potential of drilling fluids from rheological measurements. In Proceedings of the SPE/IADC Drilling Conference, Amsterdam, The Netherlands, 28 February–2 March 1995. [CrossRef]
50. Barnes, H.A.; Nguyen, Q.D. Rotating vane rheometry—A review. *J. Nonnewtonian Fluid Mech.* **2001**, *98*, 1–14. [CrossRef]
51. Fernandes, R.R.; Andrade, D.E.V.; Franco, A.T.; Negrão, C.O.R. Correlation between the gel-liquid transition stress and the storage modulus of an oil-based drilling fluid. *J. Nonnewton Fluid Mech.* **2016**, *231*, 6–10. [CrossRef]
52. Vryzas, Z.; Mahmoud, O.; Nasr-El-din, H.A.; Kelessidis, V.C. Development and testing of novel drilling fluids using Fe_2O_3 and SiO_2 nanoparticles for enhanced drilling operations. In Proceedings of the International Petroleum Technology Conference (IPTC), Doha, Qatar, 6–9 December 2015. [CrossRef]